JOC Article

Photoinduced Hinge-Like Molecular Motion: Studies on Xanthene-Based Cyclic Azobenzene Dimers

S. Anitha Nagamani, Yasuo Norikane, and Nobuyuki Tamaoki*

Molecular Smart System Group, Nanotechnology Research Institute, National Institute of Advanced Industrial Science and Technology (AIST), Tsukuba Central 5, Higashi 1-1-1, Tsukuba, Ibaraki 305-8565, Japan

n.tamaoki@aist.go.jp

Received July 1, 2005

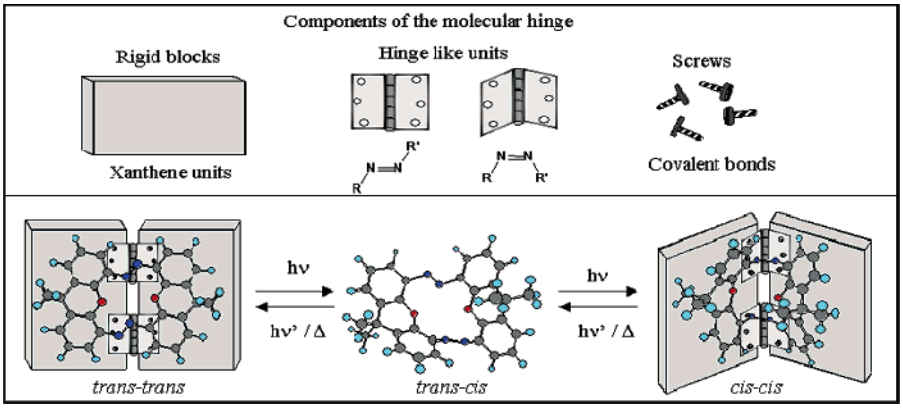

Molecular devices incorporating azobenzene units represent active components of smart systems, as they are capable of exhibiting photoregulated cooperative molecular motion. Herein, we describe the synthesis, X-ray crystal analysis, and photochemical and thermal studies of a xanthene based cyclic azobenzene dimer and its precursor. The trans−trans isomer of the azobenzene dimer upon photoirradiation transforms to the cis−cis isomer through an intermediate trans−cis isomer**.** The X-ray crystal structures of the trans−trans isomer (open) and the cis−cis isomer (closed) provide unambiguous proof for the hinge-like molecular motion in this class of molecules. The inferences drawn from photochemical and thermal studies shed light on the effect of varied substitution and cyclic structures on the different transitions. The lifetime of the cis−cis isomer is estimated to be 6.43 years, whereas the trans−cis isomer is short-lived (2.73 min) at 303 K. A rational explanation for the relative stability of the different isomers is derived from the isokinetic plot and theoretical calculations.

Introduction

The miniaturization of components used in the construction of working devices is being pursued currently by the bottom up approach, starting from the smallest compositions of matter. In this realm, chemists have extended the concept of macroscopic devices to a molecular level.[1] A molecular level device can be constructed by a single molecule or a number of molecular components that are designed so as to perform a regulated molecular motion as a consequence of appropriate external stimulation. To date, there exists many reports on two-state systems, ranging from classical cis−trans isomerization to more elaborate rotaxanes, catenanes, and biomolecular constructs.[2,3] These devices in which the molecular motion is driven by chemical, electrochemical, or photochemical forces have great potential in molecular scale information processing.

In the literature, there are reports on different kinds of molecular motions, and among them, the molecular hinge-like motion has attracted the most attention. Studies on a T4 lysozyme (an enzyme that dissolves bacterial membranes) have shown the existence of a hinge-like receptor, which controls the activity of the enzyme.[4a] The X-ray structure of a transmembrane helix having proline residues suggests that proline could

* Corresponding author. Phone: 81-298-61-4671; fax: 81-298-61-4673.

(1) Balzani, V.; Credit, A.; Raymo, F. M.; Stoddart, J. F. *Angew. Chem., Int. Ed.* **2000**, *39*, 3348−3391.

(2) Balzani, V.; Gomez, L. M.; Stoddart, J. F. *Acc. Chem. Res.* **1998**, *31*, 405−414.

(3) (a) Sauvage, J. P. *Acc. Chem. Res.* **1998**, *31*, 611−619. (b) Mao, C. D.; Sun, W. Q.; Shen, Z. Y.; Seeman, N. C. *Nature* **1999**, *397*, 144−146.

(4) (a) Dobson, C. M. *Nature* **1990**, *348*, 198−199. (b) Cordes, F. S.; Bright, J. N.; Samson, M. S. P. *J. Mol. Biol.* **2002**, *323*, 951−960. (c) Schwarzinger, S.; Wright, P. E.; Dyson, H. J. *Biochemistry* **2002**, *41*, 12681−12686.

10.1021/jo0513616 CCC: $30.25
Published on Web 10/19/2005

introduce an anisotropic molecular hinge in the helix, which is believed to assist in its channel and reception activities.[4b] Molecular hinge-like motion occurs during the protein folding of apomyglobin in its urea denatured state.[4c] Many thermally operated systems have been synthesized to mimic the functioning of the molecular hinge in biological systems. These systems that also find wide use as hosts for guest complexation use either cyclohexene, dioxa[2.2]orthocyclophane, or diazacyclohexene rings to provide the conformational flexibility.[5a−c]

It is well-known that light offers many advantages as a means for manipulating systems of either microscopic or macroscopic size. As photons can be applied with extreme temporal and spatial resolution, molecular assemblies with optical triggers are ideal systems for the construction of molecular devices. Azobenzene has been the most widely used optical trigger over the last few decades for the design and synthesis of a large variety of photoresponsive systems. This is because of the pronounced change in geometry and polarity upon its light-induced reversible isomerization, high photostability, and good quantum yields.[6]

Recently, we have reported on a novel xanthene-based cyclic azobenzene dimer, symmetrically substituted with four *t*-butyl groups exhibiting a reversible hinge-like molecular motion upon photoirradiation.[7] The two azo linkages in the trans−trans isomer photoisomerize cooperatively to form the cis−cis isomer, and this transition was intensity dependent as the intermediate trans−cis isomer was short-lived (τ = 28 s). The bulky *t*-butyl groups rendered this molecule insoluble in common organic solvents, and hence, crystallization was cumbersome. Seeking a structural modification, we present here the synthesis, characterization, photochemical, and thermal isomerization studies on an analogous cyclic azobenzene dimer and its precursor devoid of the bulky *t*-butyl groups. The purpose of this study is to first obtain the crystal structures of the trans−trans and cis−cis isomers of the cyclic azobenzene dimer, which would indeed provide unambiguous proof for the hinge-like molecular motion. Second, the unique structural feature of the cyclic azobenzene dimer is that the two azobenzene units are linked by an oxygen atom at the ortho position and a carbon atom at the meta position. The oxygen linkers bring about a conjugation throughout the cyclic structure. The noncyclic precursor has a single azobenzene unit with a similar substitution pattern. Hence, the different properties of the cyclic azobenzene dimer and its precursor are compared to reinforce the bond between molecular structure and isomerization properties in variedly substituted azobenzenes.

SCHEME 1[a]

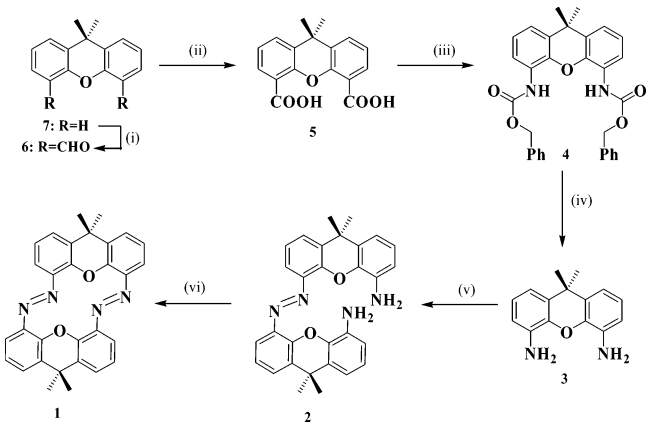

[a] (i) *n*-BuLi, dry DMF·THF, rt, 73%; (ii) Jones reagent, acetone, rt, 95%; (iii) diphenylphosphorazide, benzyl alcohol, TEA, toluene, 85 °C, 87%; (iv) KOH, EtOH, 77°C, 98%; (v) MnO_2, benzene, 80°C, 52%; and (vi) *t*-BuOK, *t*-BuOH, DMSO, rt, 17%.

Results and Discussion

(i) Synthesis. The reaction sequence adopted to synthesize the target molecules is depicted in Scheme 1. Details of the reactions are described in the Experimental Procedures. 9,9-Dimethyl xanthene was treated with *n*-BuLi/DMF in THF to yield the dialdehyde **6**,[8a] which was oxidized to the diacid **5** with Jones reagent.[8b] A Curtius reaction using diphenylphosphoryl azide in toluene transformed **5** to the rearranged dibenzyl ester **4**, which on base hydrolysis gave the key intermediate diamine **3** in quantitative yield.[8c] The diamine was oxidized in a stepwise manner to avoid polymerization. In the first step, MnO_2 oxidation gave the monoazobisamine **2(t)**, which was cyclized using *t*-BuOK to obtain the target cyclic azobenzene dimer **1(t,t)**.

(ii) Molecular Structural Details Derived from X-ray Crystal Analysis. The X-ray results of all the isomers of **1** and **2** show that the xanthene units have a nonplanar structure (bent angle = 154°), and hence, it can be fitted into an imaginary rigid block with the dimensions l = 8.5 Å, b = 5.1 Å, and w = 1.6 Å (Figure 1a).

In the case of **2**, as the two xanthene blocks are connected by one azo linkage, molecular motion along the vertical and horizontal axis of the azo linkage is allowed. Figure 1b shows the X-ray structure of the trans isomer of **2**. The torsion and dihedral angle of different bonds (Table 1) indicates nearly coplanarly arranged xanthene blocks. Thus, a part of the xanthene unit, which happens to be substituents at the 2,2′ and 3,3′ positions of the azobenzene unit, is displaced away from the adjacent ring system, thus inducing only little distortion to planarity when compared to *trans*-azobenzene.[9]

Compound **2(t)** isomerizes to give the cis isomer **2(c)** in chloroform or toluene upon exposure to 366 nm irradiation. Compound **2(c)** was isolated by silica gel

(5) (a) Ashton, P. R.; Brown, G. R.; Isaacs, N. S.; Giuffrida, D.; Kohneke, F. H.; Mathias, J. P.; Slawin, A. M.; Smith, Z. D. R.; Stoddart, J. F.; Williams, D. J. *J. Am. Chem. Soc.* **1992**, *114*, 6330−6353. (b) Mataka, S.; Mitoma, Y.; Sawada, T.; Thiemann, T.; Taniguchi, M.; Tashiro, M. *Tetrahedron* **1998**, *54*, 5171−5186. (c) Warrener, R. N.; Butler, D. N.; Liu, L.; Margetic, D.; Russell, R. A. *Chem.—Eur. J.* **2001**, *15*, 3406−3414.

(6) (a) Rau, H. *Studies in organic chemistry: Photochromism, molecules, and systems*; Durr, H., Bonas-Laurent, H. Eds.; 1990. (b) Feringa, B. L. *Molecular Switches*; Wiley VCH GmBH: Weinheim, Germany, 2001.

(7) Norikane, Y.; Tamoaki, N. *Org. Lett.* **2004**, *6*, 2595−2598.

(8) (a) Kelly, C.; Mark, V.; Vanessa, Y.; Simon, C.; Alan, F. *Biorg. Med. Chem. Lett.* **2000**, *10*, 1147−1151. (b) Dunayevskiy, Y. M.; Vouros, P.; Wintner, E. A.; Shipps, G. W.; Carell, T.; Rebek, J. *Proc. Natl. Acad. Sci. U.S.A.* **1996**, *93*, 6152−6157. (c) Buhlmann, P.; Nishizawa, S.; Xiao, K. P.; Umezawa, Y. *Tetrahedron* **1997**, *53*, 1647−1654.

(9) Bouwstra, J. A.; Schouten, A.; Kroon, J. *Acta Crystallogr.* **1983**, *C39*, 1121−1123.

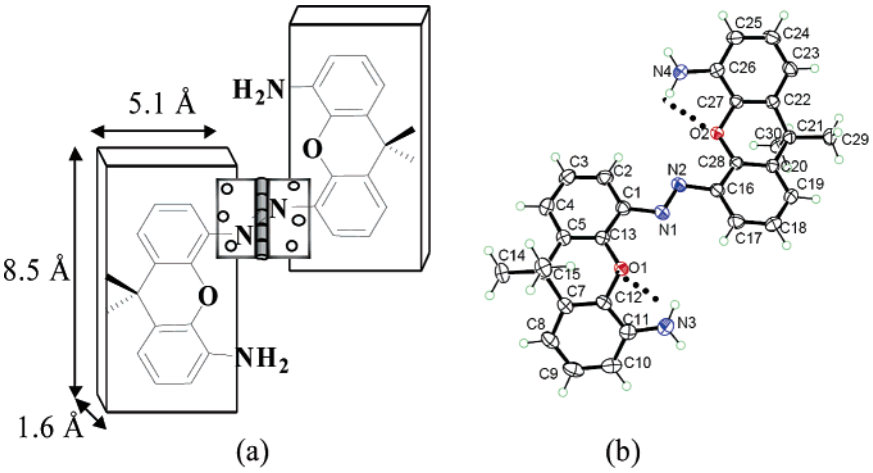

FIGURE 1. Chemical structure (a) and crystal structure of **2(t)** with displacement ellipsoids shown at the 50% probability level with the dotted lines showing the H-bonding (b).

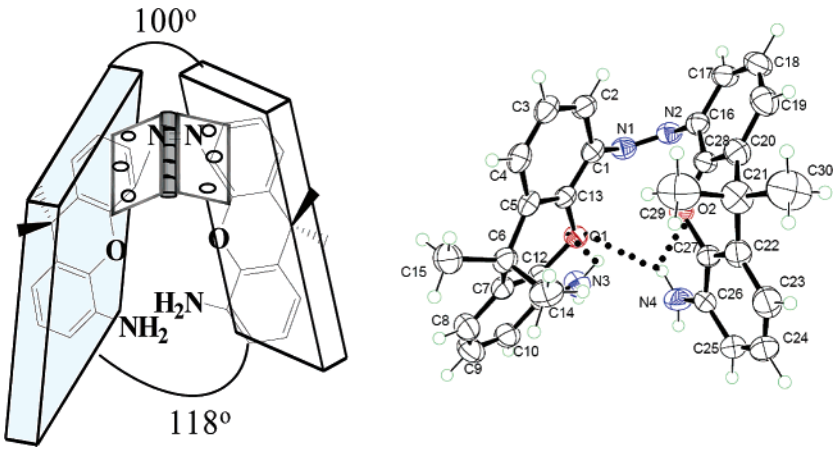

FIGURE 2. Chemical structure (a) and crystal structure of **2(c)** with displacement ellipsoids shown at the 50% probability level with the dotted lines showing the H-bonding (b).

TABLE 1. Torsion Angles and Bond Angle of Azobenzene Units in Hinge Molecule and Its Precursor

compound	type	CNNC	NNCC	NNC	CCOC
			Trans isomer		
trans-azo-benzene		180.0	17.4	114.1	
2(t)		−176.1	−176.5, 7.2 −8.2, −170.2	113.9, 113.7	146.4, −147.5 150.9, −150.2
1(t,t)	conformer A	178.9	−167.4, 14.8 −143.5, −40.1	117.0, 112.6	154.9, −156.2 26.4, −24.9
	conformer B	−179.1	31.0, −152.5 159.1, −24.4	112.3, 116.6	173.4, −175.1 −5.5, 7.8
			Cis isomer		
cis-azo-benzene		8.0	53.3	121.9	
2(c)		8.6	56.4, −131.4 55.9, −131.4	121.9, 120.9	−159.9, 156.3 150.3, −146.7
1(c,c)		−3.3	112.4, −74.2 109.3, −79.6	119.7, 120.1	151.5, 27.5 151.8, 27.1

column chromatography from an irradiated solution after attaining a photostationary state using 366 nm light. Crystallization from a mixture of chloroform and hexane gave yellow crystals suitable for X-ray analysis. The different dihedral and bond angles (Table 1) derived from the crystal structure of **2(c)** (Figure 2b) are very close to that of *cis*-azobenzene, revealing that there exists no pronounced effect of the ortho and meta substitutions.[10] The interplanar angle at the upper part of the xanthene blocks is 100°, whereas at the bottom part, it is 118° (Figure 2a), which indicates a slightly distorted overall molecular structure. In each xanthene block, there exists a H-bond between the H of the free amine and the O of the xanthene unit. An additional bond in **2(c)** is between the H of amine of one xanthene block and the O of the other xanthene block, which is in near proximity because of isomerization,[11] thus accounting for two and three H-bonds in **2(t)** and **2(c)**, respectively. This opportunity

(10) Mostad, A.; Romming, C. *Acta Chem. Scand.* **1971**, *25*, 3561–3568.

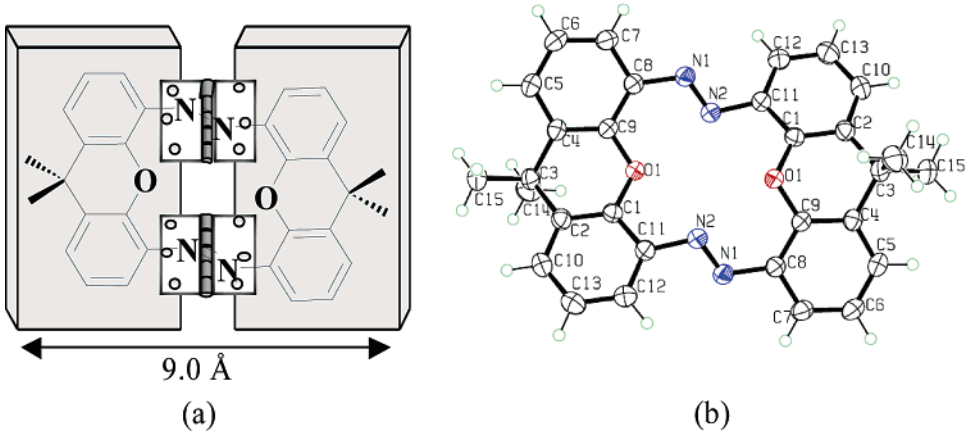

FIGURE 3. Chemical structure (a) and crystal structure of **1(t,t)** conformer A with displacement ellipsoids shown at the 50% probability level (b).

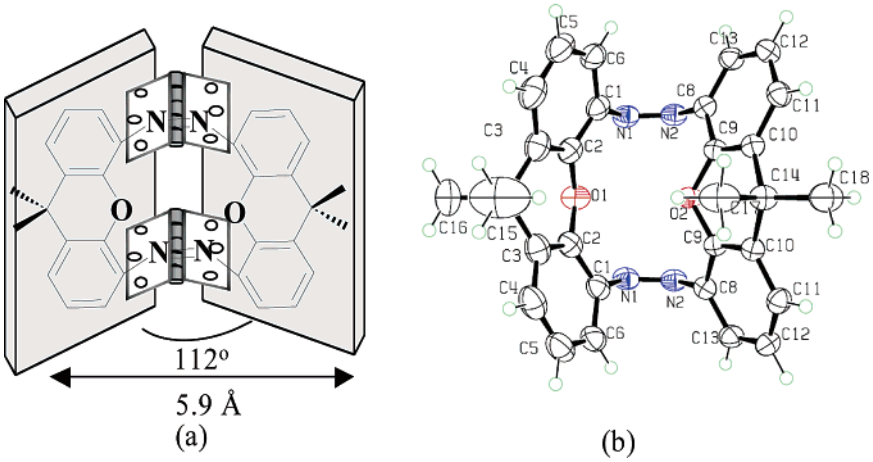

FIGURE 4. Chemical structure (a) and crystal structure of **1(c,c)** with displacement ellipsoids shown at the 50% probability level (b).

for the formation of an additional H-bond may be the driving force for the stabilization of the present conformation in **2(c)** over the one in which the amino groups are oriented in opposite directions.

In the case of **1**, two azo linkages are used for connecting the two xanthene blocks. Efficient motion of the two azo linkages must occur in a cooperative fashion along the vertical axis to bring about the unique hinge-like molecular motion between the **1(t,t)** and **1(c,c)** isomers. X-ray crystal analysis of **1(t,t)** revealed that there are two kinds of conformers in a unit cell. They mainly differ in the extent of bending at the xanthene units and hence vary in the length and width of the xanthene blocks (conformer A: $l = 8.5$ Å and $w = 1.6$ Å; conformer B: $l = 9.0$ Å and $w = 0.9$ Å). Figure 3b shows the X-ray structure of conformer A, and the representative bond angles are compiled in Table 1. The torsional angle s for —N=N— bonds in both the conformers is 179°, thus steering the two xanthene blocks to coplanarity.

The lifetime of **1(c,c)** was long enough for isolation and crystallization. Compound **1(t,t)** isomerized to give **1(t,c),** which further isomerized to **1(c,c)** in chloroform or toluene upon exposure to 366 nm irradiation. Compound **1(c,c)** was isolated by silica gel column chromatography from an irradiated solution after attaining photostationary state using 366 nm light. Crystallization from a mixture of dichloromethane and hexane gave orange crystals suitable for X-ray analysis. In **1(c,c)** (Figure 4b), the two azobenzene units were placed in a cyclic structure without bringing about much change in the C—N=N angles (120°) or the C—N=N—C dihedral angle (−3.3°) as compared to that of *cis*-azobenzene. The molecule has a mirror plane passing through the center of the xanthene unit. The interplanar angle between the two xanthene blocks is 112° (Figure 4a), which confirms the uniformly bent structure of **1(c,c)**. The crystal structures of **1(t,t)** and **1(c,c)**, which represent the open and closed states, provide unambiguous proof for the hinge-like molecular motion (Figures 3a and 4a). The distance between the carbon atoms at the para-positions of both the azobenzene units in **1(t,t)** is 9.0 Å, and the same in **1(c,c)** is 5.9 Å, thus leading to a 35% reduction in the

(11) Jeffrey, G. A.; Saenger, W. *Hydrogen Bonding in Biological Structures*; Springer-Verlag: Berlin, 1991. The H-bonds have been identified based on the distance between the proton and the acceptor (i.e., d(H···O)) and the angle made between the donor—proton—acceptor atoms (i.e., θ(N—H···O)). H-bonds are present between a H (H3 and H4) of the free amine and the O (O1 and O2) of the xanthene unit, and the distance d(H···O) is 2.33 Å and the angle θ(N—H···O) is 103° in both **2(t)** and **2(c).** The additional H-bond in **2(c)** has d(H···O) of 2.45 Å and an angle θ(N—H···O) of 136°.

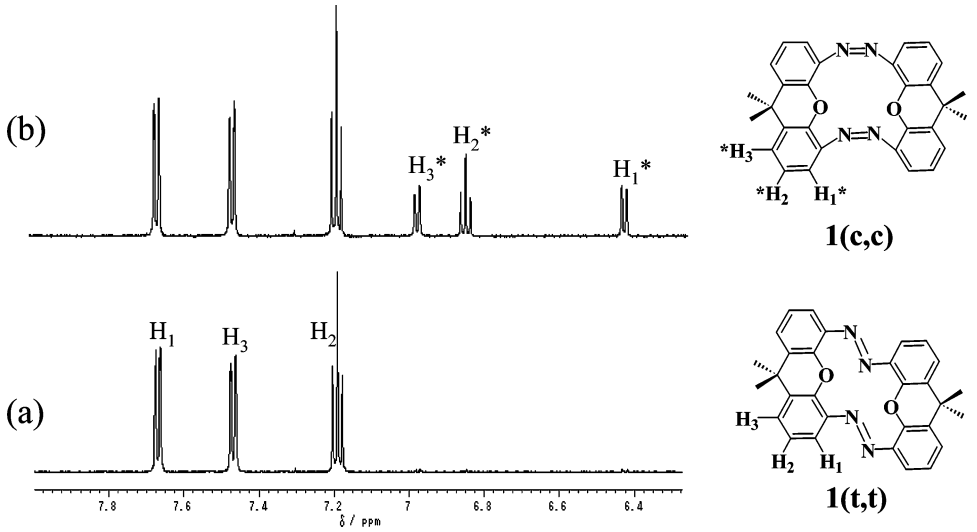

FIGURE 5. ^{1}H NMR spectra of **1(t,t)** in 1,1,2,2-tetrachloroethane-d_2 before (a) and after (b) irradiation. For labeling, see the structures of **1(t,t)** and **1(c,c)** given beside the spectra.

length of the molecule. These two states are reversible on photoirradiation and have a high thermal stability as the azo linkages act cooperatively to stabilize the respective configurations.

(iii) NMR Spectral Changes. NMR assignments clearly indicate a difference in chemical shifts between the proton resonances of the cis and trans isomers, which are expected from an empirical standpoint.[12] The reasons are the following: (i) the two aromatic rings are initially remote from one another (trans) but encounter each other closely as a result of photoisomerization (cis) and (ii) protons that were initially only subject to the local deshielding effect of their own aromatic ring within the ring plane (trans) now encounter the additional shielding effect of the remote out-of-plane aromatic ring (cis). The NMR spectral changes obtained for **2** after irradiation are similar to several substituted azobenzenes (see Supporting Information for details).

Figure 5a shows the ^{1}H NMR spectrum of **1** (in 1,1,2,2-tetrachloroethane-d_2) in the aromatic region, which can be attributed to a single form of the molecule **1(t,t)**. On the basis of symmetry considerations, the two doublets at 7.66 and 7.46 ppm representing the two sets of two aromatic protons belong to the H_1 and H_3 protons, and a triplet at 7.18 ppm integrating for one set of two aromatic protons belongs to the H_2 protons. The spectrum obtained upon photoirradiation with 366 nm light for 5 min is as shown in Figure 5b. The signals corresponding to **1(c,c)** appear upfield as compared to that of the **1(t,t)**, and signals corresponding to the short-lived isomer **1(t,c)** were not observed. A doublet at 6.97 ppm integrating for one set of two aromatic protons belongs to the H_3* protons, one triplet at 6.83 ppm integrating for one set of two aromatic protons belongs to the H_2* protons, and one doublet at 6.41 ppm integrating for one set of two aromatic protons belongs to the H_1* protons. Integration of the signals corresponding to **1(t,t)** and **1(c,c)** gives a composition of 80% of **1(t,t)** and 20% of **1(c,c)**.

In **1**, the aliphatic (methyl) protons appear as singlets in both trans and cis isomers, indicating that these are least affected by the isomerization because of their greater distance and lack of conjugation from the azo unit. In general, the protons at the ortho position of the azo group have maximum shift as compared to that of the meta or para positions. In **1(c,c)**, the ortho protons are shifted upfield by 1.25 ppm, whereas the meta and para protons are shifted approximately by 0.4 ppm, which concurs with the values obtained for several substituted azobenzenes.

(iii) Absorption Spectra. Figures 6a and 7a show the absorption spectra of **2(t)** and **1(t,t)** in toluene, respectively. The absorption maxima of **2(t)** are 395 nm (ϵ = 8000 M^{-1} cm^{-1}) and 326 nm (ϵ = 11 000 M^{-1} cm^{-1}), while those of **1(t,t)** are 365 nm (ϵ = 15 000 M^{-1} cm^{-1}) and 320 nm (ϵ = 29 000 M^{-1} cm^{-1}). The absorption spectra of the trans isomers of both the compounds are similar, and they differ from that of azobenzene itself, which exhibits absorption maxima at 444 nm ($n-\pi^*$, ϵ = 440 M^{-1} cm^{-1}) and 316 nm ($\pi-\pi^*$, ϵ = 22 000 M^{-1} cm^{-1}).[13] The cyclic structure brings about a hypsochromic shift for both the $\pi-\pi^*$ bands as compared to the acyclic analogue. The molar extinction coefficient of **2(t)** is almost half of that of **1(t,t)**, which is reasonable as **2(t)** has only one azobenzene unit, whereas in **1(t,t)** two azobenzene units form the cyclic structure. The molar extinction coefficient of azobenzene for the $\pi-\pi^*$ transition seems to be intermediate to that of **2(t)** and **1(t,t)**, indicating that the specific substitution pattern influences the electronic and steric interactions, thus affecting the absorption. The special features of the absorption spectra of **1(t,t)** are the splitting of the $\pi-\pi^*$ band and the absence of any distinct $n-\pi^*$ band. Upon photoirradiation, there is a decrease in the absorption of both the $\pi-\pi^*$ bands without any concomitant increase in the $n-\pi^*$ band. Normally for azobenzene, the spectra are characterized by a low intensity (symmetry forbidden) $n-\pi^*$ band in the 400−500 nm region and a very intense (symmetry allowed)

(12) Tait, K. M.; Parkinson, J. A.; Bates, S. P.; Ebenezer, W. J.; Jones, A. C. *J. Photochem. Photobiol., A* **2003**, *154*, 179−188.

(13) Forber, C. L.; Kelusky, E. C, Bunce, N. J.; Zerner, M. C. *J. Am. Chem. Soc* **1985**, *107*, 5884−5890.

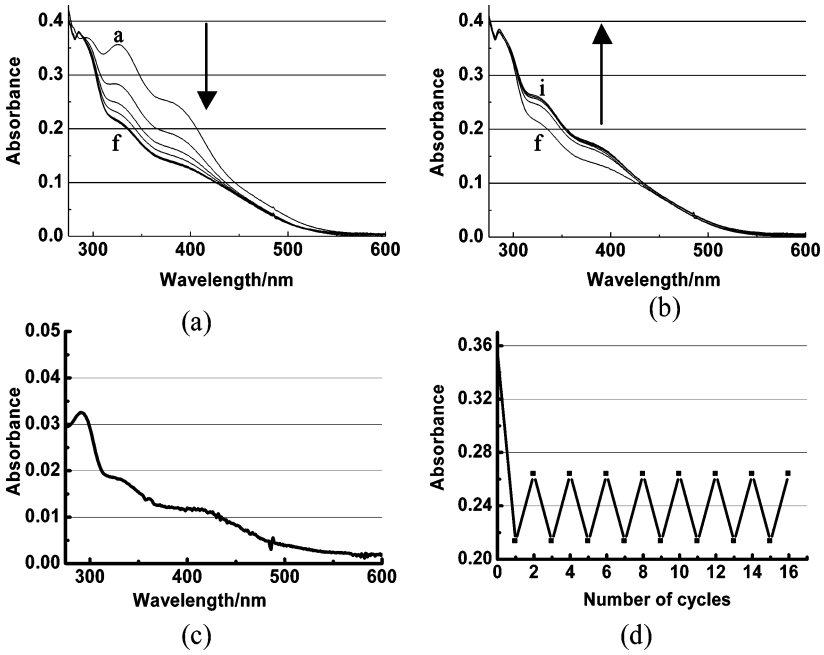

FIGURE 6. Changes in the absorption spectra of **2(t)** in toluene upon irradiation at (a) 366 nm: a, 0 min; b, 20 s; c, 40 s; d, 1 min; e, 1.5 min; and f, 2 min. (b) 436 nm: f, 0 min; g, 10 s; h, 20 s; and i, 30 s. (c) Absorption spectra of pure **2(c)** measured by a photodiode array detector attached to a HPLC system. (d) Absorption changes observed at 326 nm after alternating the irradiations at 366 nm (3 min) and 436 nm (1 min) over 16 complete cycles.

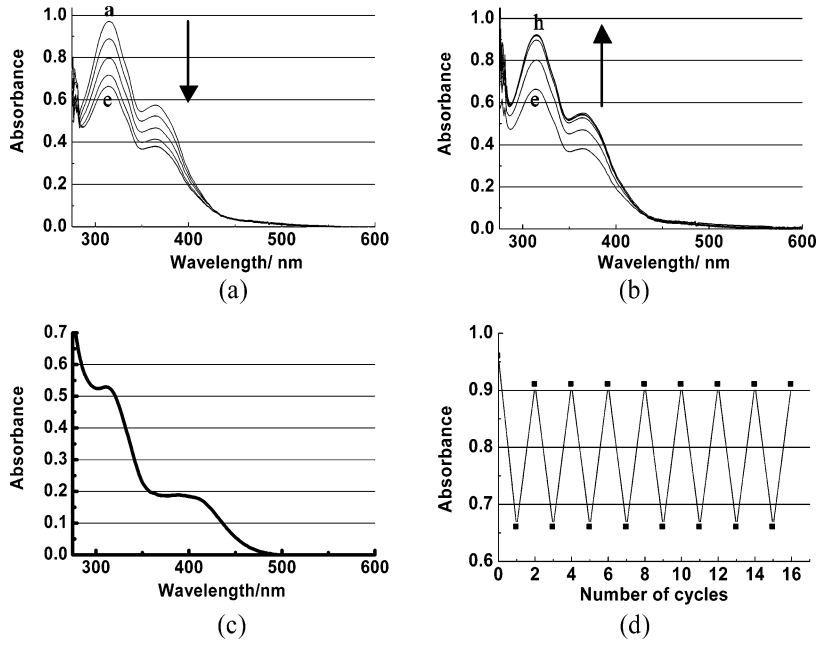

FIGURE 7. Changes in the absorption spectra of **1(t,t)** in toluene upon irradiation at (a) 366 nm: a, 0 min; b, 2 min; c, 3 min; d, 5 min; and e, 7 min. (b) 436 nm: e, 0 min; f, 30 s; g, 1 min; and h, 2 min. (c) Absorption spectra of pure **1(c,c)** measured by a photodiode array detector attached to a HPLC system. (d) Absorption changes observed at 320 nm after alternating the irradiations at 366 nm (8 min) and 436 nm (3 min) over 16 complete cycles.

$\pi-\pi^*$ band at the 300−340 nm region. Upon photoirradiation as a consequence of trans−cis isomerization, the intensity of the $\pi-\pi^*$ band is decreased with a concomitant increase of that of the $n-\pi^*$ band.

Usually, all azobenzenophanes have an auxiliary band of moderate intensity in the 380 nm region, Rottger et al. attributed the origin of these bands to the interactions of the transition moments.[14] Figure 7a,b shows that the auxiliary band in the present case is more distinct when compared to that of other azobenzenophanes. As a similar spectral pattern and changes are observed in the noncyclic **2(t)** (Figure 6a,b), one can rule out the role of a cyclic structure in bringing out such an effect. So, the specific substitution on the azobenzene unit plays a major role. In most of the reported cyclic azobenzene dimers,

(14) Rottger, D.; Rau, H. *J. Photochem. Photobiol., A* **1996**, *101*, 205−214.

the azobenzene units are connected through one or more insulating methylene units; thus, the azobenzene units act independently.[15] In the present case, each azobenzene unit acts as a substituent on the other because they are conjugated through the ortho oxygen linkers. 2,2′-Dimethoxyazobenzene exhibits a typical splitting of the $\pi-\pi^*$ band and is explained based on the steric inhibition to planarity in these systems, which arises because of the bulky ortho substituent.[16] But, the X-ray results of **1(t,t)** and **2(t)** show that the azobenzene units are not distorted from planarity to a large extent. So, it is probable that the splitting of the $\pi-\pi^*$ band in the absorption spectra stems from the electronic effect of the ortho oxygen substituent as suggested by Morris and Brode.[17] Figures 6c and 7c show the absorption spectra of the pure cis isomers **2(c)** and **1(c,c)** in toluene, respectively. It is evident that the peak positions of the cis isomers are similar to that of the trans isomers. So, it is perceivable that at the photostationary state the absorption of the trans isomer dominates, and the spectra of the trans rich and cis rich states differ only in the absorption intensity.

(iv) Photochemical Isomerization. The absorption spectral changes that occur for **2(t)** and **1(t,t)** on photoisomerization are as shown in Figures 6a,b and 7a,b. Both compounds behave in a similar manner. Upon irradiation with 366 nm light, there is a gradual decrease in the intensity of absorption of both the $\pi-\pi^*$ bands, and upon irradiation with 436 nm light, the absorption intensity is recovered back (52% for **2(t)** and 95% for **1-(t,t)**). The photostationary state composition was determined using NMR analysis. Compound **2(t)** upon 366 nm irradiation isomerizes to **2(c)**, yielding a photostationary state composition of 26% of **2(t)** and 73% of **2(c)** within 2 min. Compound **1(t,t)** isomerizes to **1(t,c),** which further isomerizes to **1(c,c)**, and a photostationary state composition of 67% of **1(t,t)** and 32% of **1(c,c)** was reached within 7 min. The recovery of **2(t)** from **2(c)** by 436 nm irradiation is much lower than that of **1(t,t)** from **1(c,c)**, probably because of (i) a higher quantum yield of the forward isomerization and (ii) a higher molar extinction coefficient of **2(t)**. By alternating the irradiation wavelengths between 366 and 436 nm, we verified that the photochemical trans−cis and cis−trans processes could be repeated between the 366 and 436 nm photostationary states for more than 16 cycles (Figures 6d and 7d).

The photoisomerization quantum yields can be calculated by the temporal absorption spectra if the absorption coefficients of the reacting molecules are known. As described earlier with help of ^{1}H NMR spectral data, the composition of the isomers at the 366 nm photostationary state was estimated. The extinction coefficient of **2(c)** was estimated to be 5000 M^{-1} cm^{-1} (326 nm) and 3600 M^{-1} cm^{-1} (395 nm), and that for **1(c,c)** was 3800 M^{-1} cm^{-1} (365 nm) and 7200 M^{-1} cm^{-1} (320 nm). As the intermediate **1(t,c)** was short-lived, an accurate calculation of its concentration and hence its molar extinction coefficient was not feasible. Assuming that azobenzene units absorb independently in **1(t,c)**, we calculated the ϵ of **1(t,c)** as an average value of the molar extinction coefficients of **1(t,t)** and **1(c,c)**; hence, ϵ of **1(t,c)** at 365 nm was 9400 M^{-1} cm^{-1} and at 320 nm was 18 000 M^{-1} cm^{-1}. Making use of these values of molar extinction coefficients and the initial portion of the A_{320} and time plots, the quantum yields were evaluated. For the cyclic azobenzene dimer, Φ_{tt-tc} was evaluated to be 0.01, whereas for its precursor, Φ_{t-c} was found to be 0.16. The lower value of the quantum yield for the cyclic azobenzene dimer may be due to (i) the lack of an apparent energy minimum for the different transition state geometries between **1(t,t)** and **1(t,c)** and (ii) probably the isomerization is through a transition state having close resemblance to **1(t,t)** geometry.

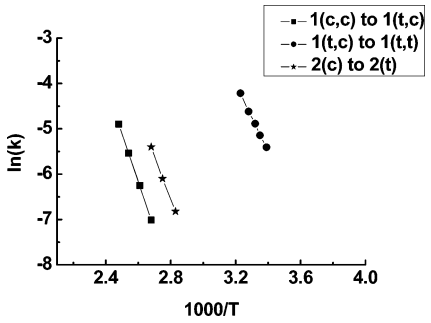

FIGURE 8. Comparison of the rate constants of the different transitions for **1** and **2**.

(v) Thermal Isomerization. The thermal cis−trans isomerization of the transition **2(c)** to **2(t)** was determined by monitoring the increase of absorbance at λ_{max} in the absorption spectra. The first-order rate constant (k) of the reaction was found to be 1.3×10^{-5} s^{-1} at 303 K. Compound **1(c,c)** isomerizes in a stepwise manner, initially to **1(t,c)**, which further isomerizes to **1(t,t)**. The transition from **1(c,c)** to **1(t,c)** is very slow and proceeds with a first-order rate constant $k = 5.01 \times 10^{-9}$ s^{-1} at 303 K, which was monitored by the temporal increase in concentration of **1(t,t)** with temperature by NMR analysis. Compound **1(t,c)** isomerizes very quickly to **1(t,t)** with a first-order rate constant $k = 8.53 \times 10^{-3}$ s^{-1} at 303 K, which was independently determined by following the increase of absorbance at λ_{max} within 5 min just after 366 nm irradiation using a photodiode array detector. The first-order rate plots of these transitions at different temperatures (Figure 8) were used to calculate the thermodynamic parameters of the back relaxation process, namely, the activation energy (E_a), Arrhenius parameter (A), activation enthalpy ($\Delta H^{\ddagger}$), the activation entropy ($\Delta S^{\ddagger}$), and the Gibbs free energy of activation ($\Delta G^{\ddagger}$). The values obtained for the different parameters are tabulated (Table 2).

The thermodynamic parameters for the transition to **2(t)** are comparable to that of cis−trans isomerization

(15) (a) Norikane, Y.; Kitamoto, K.; Tamaoki, N. *J. Org. Chem.* **2003**, *68*, 8291−8304. (b) Tamaoki, N.; Koseki, K.; Yamaoka, T. *Angew. Chem., Int. Ed. Eng.* **1990**, *29*, 105−106. (c) Tamaoki, N.; Ogata, K.; Koseki, K.; Yamaoka, T. *Tetrahedron* **1990**, *46*, 5931−5942. (d) Tamaoki, N.; Yamaoka, T. *J. Chem. Soc., Perkin. Trans.* **1991**, 873−878. (e) Tamaoki, N.; Yoshimura, S.; Yamaoka, T. *Thin Solid Films* **1992**, *221*, 132−139. (f) Rau, H.; Rottger, D. *Mol. Cryst. Liq. Cryst.* **1994**, *246*, 143−146. (g) Tauer, E.; Machinek, R. *Liebigs Ann.* **1996**, 1213−1216. (h) Luboch, E.; Wagner-Wysiecka, V. C.; Kravtsov; Kessler, V. *Pol. J. Chem.* **2003**, *77*, 189−196.

(16) Gore, P. H.; Wheeler, O. H. *J. Am. Chem. Soc.* **1961**, *26*, 3295−3298.

(17) Morris, R. J.; Brode, W. R. *J. Am. Chem. Soc.* **1948**, *70*, 2485−2488.

TABLE 2. Thermodynamic Properties for the Different Transitions of 1 and 2

transition	E_a (kcal mol^{-1})	A	ΔH (kcal mol^{-1})	ΔS (cal K^{-1} mol^{-1})	ΔG (kcal mol^{-1})	$\tau = 1/k$ at 303 K
2(c) to **2(t)**	18.5	3.2×10^8	17.9	−8.38	21.0	20.6 h
1(t,c) to **1(t,t)**	14.3	1.7×10^8	13.7	−9.15	16.4	2.73 min
1(c,c) to **1(t,c)**	22.0	2.3×10^8	21.2	−4.25	22.5	6.43 years

of several 2,2′-disubstituted azobenzenes.[18] The thermal isomerization of **1(t,c)**−**1(t,t)** is 10 00 000 times faster than **1(c,c)**−**1(t,c)**. This is mainly due to the extremely low activation energy (E_a = 14.3 kcal mol^{-1}). The entropy of activation is higher for the transition **1(c,c)**−**1(t,c)** as compared to that of **1(t,c)**−**1(t,t)**, which indicates a modestly increased disorder at the transition state. Compound **2(c)** has a lifetime (τ) of 20.6 h (*1/k*) at 303 K. The most striking feature of **1** is that **1(c,c)** has the longest lifetime (τ) of 6.43 years (*1/k*) at 303 K among the known cyclic azobenzene dimers.[19] The lifetime of the **1(t,c)** isomer devoid of the bulky *t*-butyl groups has increased 8-fold as compared to the trans−cis isomer having *t*-butyl groups indicating the major role played by steric crowding in destabilizing the isomer.

A theoretical support was sought to evaluate the relative stability of all the isomers of **1** and **2**, and the heats of formation were estimated by ab initio quantum chemical calculations using the RHF/6-31G** method.[19] The geometries of the molecular structures were fully optimized. The calculations for **2** show that **2(t)** is 10.0 kcal mol^{-1} more stable than **2(c)**. An experimental study on the heat of combustion showed that *trans*-azobenzene is about 10.0 kcal mol^{-1} more stable than *cis*-azobenzene.[20] The values predicted for **2** match well with that of azobenzene. The results pertaining to **1** (Figure 9) show that **1(t,t)** and **1(c,c)** are 26.7 and 1.24 kcal mol^{-1} more stable than **1(t,c)**. The relatively small energy difference between **1(t,c)** and **1(c,c)** and an extraordinarily large energy difference between **1(t,t)** and **1(t,c)** indicates that **1(t,c)** may be destabilized by its distorted structure conferred by the ring strains.

To compare the mechanism of thermal isomerization, a general isokinetic plot or compensation rule is used, which translates into a linear interdependence of $\Delta H^{\ddagger}$ and $\Delta S^{\ddagger}$. This particular trend is followed when isomerization occurs via a common mechanism.[21] Figure 10 shows the isokinetic plot for **1**, **2**, azobenzene, and its dimers for which the thermodynamic properties are reported. It is interesting to note that in all the compounds except for the two points, which correspond to the **(t,c)**−**(t,t)** process of **1** and that of the dibenzo-

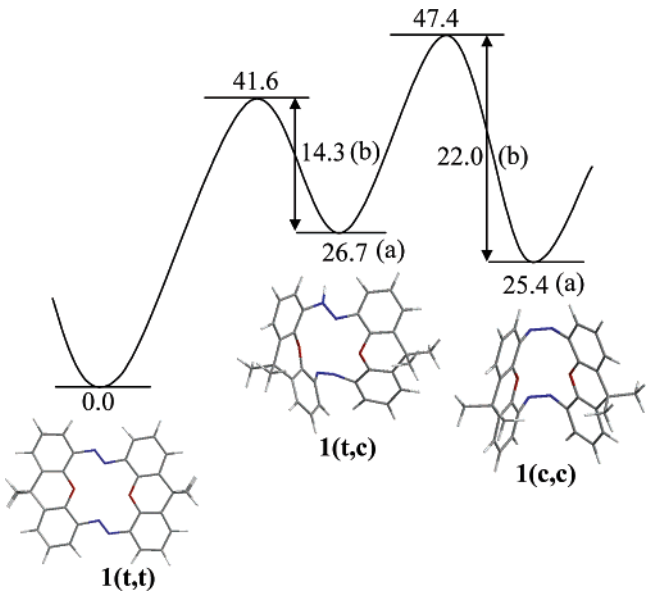

FIGURE 9. Energy diagram of **1** estimated from the experiment and theoretical calculations. Structures shown were obtained from RHF/6-31G** calculations: (a) values calculated theoretically and (b) experimental values.

azobenzenophanes, the compensation rule has been found. The line corresponds to the various azobenzenes that have been reported to isomerize by the inversion mechanism. Scattering of the values around the straight line is due to the effect of steric crowding and solvation on rate. Thus, the inversion mechanism may be operative in the thermal back relaxation of **1(c,c)**−**1(t,c)** and **2(c)**−**2(t)** transitions.

But, the **(t,c)** to **(t,t)** transitions of **1** and **11** seem to proceed by a different mechanism. The steric distortion of **(t,c)** isomers of these systems is very high as the two azobenzene units, one in the trans form (9.0 Å) and the other in cis form (5.9 Å), have the restrictions of both distance and angle imposed by the central pyran or phenyl ring. As the isomerization starts from a trans−cis isomer having a highly distorted structure, it can be expected to opt for a different kind of mechanism for the transition to get rid of the steric strains. Thus, the thermodynamic parameters fall apart from the common straight line representing the inversion mechanism.

Conclusions

We have provided unambiguous proof for the photoinduced hinge-like molecular motion using the X-ray crystal structures of **1(t,t)** (open) and **1(c,c)** (closed) states. The two azo linkages in **1(t,t)** cooperatively isomerize to **1(c,c)** via a short-lived **1(t,c)** isomer. The thermal isomerization of **1(t,c)**−**1(t,t)** was found to be 10 00 000 times faster than **1(c,c)**−**1(t,c)**. The lifetime of **1(c,c)** was estimated to be 6.43 years; thus, **1(c,c)** is the longest lived cis−cis isomer of cyclic azobenzene

(18) Nishimura, N.; Sueyoshi, T.; Yamanaka, H.; Imai, E.; Yamamoto, S.; Hasegawa, S. *Bull. Chem. Soc. Jpn.* **1976**, *49*, 1381−1387.
(19) Frisch, M. J.; Trucks, G. W.; Schlegel, H. B.; Scuseria, G. E.; Robb, M. A.; Cheeseman, J. R.; Zakrzewski, V. G.; Montgomery, J. A.; Stratmann, R. E.; Burant, J.; Dapprich, S. C.; Millam, J. M.; Daniels, A. D.; Kudin, K. N.; Strain, M. C.; Farkas, O.; Tomasi, J.; Barone, V.; Cossi, M.; Cammi, R.; Mennucci, B.; Pomelli, C.; Adamo, C.; Clifford, S.; Ochterski, J.; Petersson, G. A.; Ayala, P. Y. C.; Morokuma, K. Q.; Malick, D. K.; Rabuck, A. D.; Raghavachari, K.; Foresman, J. B.; Cioslowski, J.; Ortiz, J. V.; Baboul, A. G.; Stefanov, B. B.; Liu, G.; Liashenko, A.; Piskorz, P.; Komaromi, I.; Gomperts, R.; Martin, R. L.; Fox, D. J.; Keith, T.; Al-Laham, M. A.; Peng, C. Y.; Nanayakkara, A.; Challacombe, M.; Gill, P. M. W.; Johnson, B. C.; Wong, M. W.; Andres, J. L. W.; Gonzalez, C.; Head-Gordon, M.; Replogle, E. S.; Pople, J. A. *Gaussian 98, Revision A.9;* Gaussian, Inc: Pittsburgh, PA 1998.
(20) Corruccini, R. J.; Gilbert, E. C. *J. Am. Chem. Soc.* **1939**, *61*, 2925−2927.
(21) Asano, T.; Okada, T.; Shinkai, S.; Shigematsu, K.; Kusano, Y.; Manabe, O. *J. Am. Chem. Soc.* **1981**, *103*, 5161−5165.

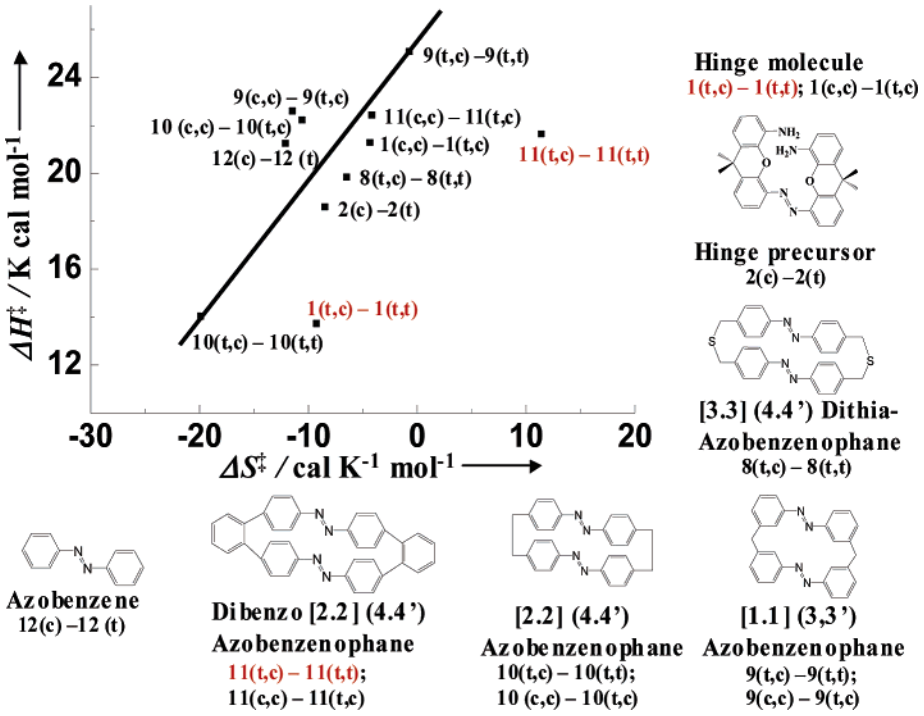

FIGURE 10. Isokinetic plot for $\Delta H^{\ddagger} - \Delta S^{\ddagger}$ of the cis−trans thermal isomerization of cyclic azobenzene dimers.

dimers. The photochemical and thermal behavior of **2** is similar to several 2,2′-disubstituted azobenzenes. Quantum chemical calculations predict a relatively small energy difference between **1(t,c)** and **1(c,c)**, indicating that **1(t,c)** may be destabilized by its highly distorted structure conferred by the ring strains. The isokinetic plot revealed that the thermal isomerization of **2(c)**−**2(t)** and **1(c,c)**−**1(t,c)** followed inversion mechanisms, whereas the transition **1(t,c)**−**1(t,t)** proceeded by a different mechanism. The cyclic structure restricts the rotation of the phenyl units around the azo linkages, thus regulating the motion of the molecular device. Thus, the knowledge of correlation between the structure and the isomerization property of variedly substituted azobenzenes can make way for the better design of photoregulated molecular devices.

Experimental Procedures

9,9-Dimethyl-9*H*-xanthene-4,5-dicarbaldehyde (6). *n*-Butyllithium (7.4 mL, in hexane, 11.9 mmol) was added dropwise to a stirred and cooled solution of 9,9-dimethyl-9*H*-xanthene (1 g, 4.76 mmol) in dry THF (50.0 mL) under an atmosphere of dry nitrogen. The reaction mixture was stirred at room temperature for 15 min, and then a previously cooled solution of DMF (0.9 mL, 11.9 mmol) in THF (4.0 mL) was added dropwise at 0 °C. The reaction mixture was slowly allowed to warm to room temperature and was stirred for 1 h, and then diluted HCl (10.0 mL) was added. The reaction mixture was then taken up in ether (2 × 50 mL), and the combined ether extracts were washed with water (2 × 50 mL) and dried over anhydrous sodium sulfate. The solvent was removed in vacuo, and the pure product was isolated by column chromatography on silica gel with hexane/ethyl acetate (9:1) as eluent. The pure product was obtained as an off-white solid. Yield = 73%; mp = 178−182 °C; ^{1}H NMR (300 MHz, $CDCl_3$): δ 10.69 (s, 2H, 2 × CHO), 7.82 (dd, J_1 = 7.5 Hz, J_2 = 1.6 Hz, 2H, Ar), 7.71 (dd, J_1 = 7.5 Hz, J_2 = 1.6 Hz, 2H, Ar), 7.26 (t, J = 7.7H, 2H, Ar), 1.69 (s, 6H, 2 × CH_3).

9,9-Dimethyl-9*H*-xanthene-4,5-dicarboxylic Acid (5). Freshly prepared Jones reagent was added dropwise to a solution of **6** (1 g, 3.73 mmol) in acetone (10.0 mL) until the reddish brown color persisted. The reaction mixture was stirred at room-temperature overnight. Addition of water (10.0 mL) led to precipitation of the product as a white solid, which was filtered and dried. Yield = 95%, mp = 248 °C; ^{1}H NMR (300 MHz, $CDCl_3$): 7.79 (dd, J_1 = 7.7 Hz, J_2 = 1.2 Hz, 2H, Ar), 7.69 (dd, J_1 = 7.7 Hz, J_2 = 1. 2 Hz, 2H, Ar), 7.25 (t, J = 7.7H, 2H, Ar), 1.61 (s, 6H, 2 × CH_3).

9,9-Dimethyl-9*H*-xanthene-4,5-diylbiscarbamic Acid Dibenzyl Ester (4). Compound **5** (1 g, 3.2 mmol), diphenylphosphorazide (0.7 g, 6.6 mmol), triethylamine (0.68 g, 6.6 mmol), benzyl alcohol (0.72 g, 6.66 mmol), and toluene (40.0 mL) were heated at 80 °C for 22 h. Upon evaporation of the solvent, a pale yellow oil was obtained that was purified on a silica gel column using hexane/ethyl acetate (9:1) as the eluent to yield the product as a white crystalline solid. Yield = 87%; mp =110−112 °C; ^{1}H NMR (300 MHz, $CDCl_3$): 8.03 (brs, 2 H, 2 × NH), 7.36−7.05 (m, 16H, Ar), 5.14 (s, 4H, 2 × CH_2Ph), 1.60 (s, 6H, 2 × CH_3).

9,9-Dimethyl-9*H*-xanthene-4,5-diamine (3). Compound **4** (1 g, 2.1 mmoles) was dissolved in EtOH (100 mL) saturated with KOH and heated to 100 °C for 24 h. After neutralizing the reaction mixture, the product was extracted into ethyl acetate. The organic layer was dried over sodium sulfate and evaporated to give a brown solid, which was purified on a silica gel column using hexanes/ethyl acetate (4:1) as an eluent to afford the product as light yellow solid. Yield = 98%; mp =148−151 °C; ^{1}H NMR (300 MHz, $CDCl_3$): 6.91 (t, J = 7.7 Hz, 2H, Ar), 6.84 (dd, J_1 = 7.4 Hz, 2H, Ar), 6.65 (dd, J_1 = 7.6 Hz, J_2 = 1.7 Hz, 2H, Ar), 3.84 (brs, 4H, 2 × NH_2), 1.6 (s, 6H, 2 × CH_3).

(*E*)-1,2-Bis(5-amino-9,9-dimethyl-9H-xanthene-4-yl)-diazene (2). A benzene solution (200 mL) of a mixture of **3** (1.20 g, 3.40 mmol) and MnO_2 (1.5 g) was refluxed in the dark for 45 h. After cooling to room temperature, the reaction mixture was filtered through Celite. The filtrate was evaporated to dryness under reduced pressure, and the residue was chromatographed on silica gel with hexane/ethyl acetate (9:1) as eluent, to give **2** purely in its trans form as an orange solid.

Yield = 52%; mp = >300 °C; ^{1}H NMR (600 MHz, $CDCl_3$): 7.66 (dd, J_1 = 8.6 Hz, J_2 = 2.4 Hz, 2H, Ar), 7.55 (dd, J_1 = 7.5 Hz, J_2 = 1.2 Hz, 2H, Ar), 7.16 (t, J = 8.0 Hz, 2H, Ar), 6.95 (t, J = 8.0 Hz, 2H, Ar), 6.84 (d, J = 8.1 Hz, 2H, Ar), 6.68 (d, J = 8.2 Hz, 2H, Ar), 4.11(brs, 4H, 2 × NH_2) and 1.69 (s, 6H, 2 × CH_3) ^{13}C NMR (75 MHz, $CDCl_3$): 147.8 (C), 141.3 (C), 138.3 (C), 135.3 (C), 132.6 (C), 130.3 (C), 128.6 (CH), 123.5 (CH), 122.7 (CH), 115.9 (CH), 114.6 (CH), 113.3 (CH), 34.5 (C), 31.6 (CH_3). ESIMS (*m/z*) [M + H] calcd for $C_{30}H_{28}O_2N_4$ 477.52, found 477.41.

(*E,E*) 1,16-Dioxa[1.1.1.1](2,2′,3,3′)31,31,32,32 Tetramethyl Azobenzenophane (1). In the presence of dry oxygen, potassium *t*-butoxide (32 mg, 0.28 mmol) in DMSO and *t*-butyl alcohol (25 mL, 80:20) was vigorously stirred. From a dropping funnel, **2** (50 mg, 0.071 mmol) in a mixture of DMSO and *t*-butyl alcohol (25 mL, 80:20) was slowly added for 3 h at room temperature. After stirring at room temperature for 40 h, the reaction mixture was poured into ice water. Dilute hydrochloric acid (10.0 mL) was added and extracted by chloroform. The organic layer was washed by water and saturated with NaCl solution. The organic layer was dried over anhydrous $MgSO_4$ and evaporated to dryness under reduced pressure. The residue was chromatographed on silica gel with hexane/chloroform (3:2) as eluent, to give **1** purely in its trans−trans form as a yellow solid. Yield in 17%; mp = >300 °C; ^{1}H NMR (600 MHz, $CDCl_3$): 7.79 (dd, J_1 = 7.9 Hz, J_2 = 1.6 Hz, 4H, Ar), 7.55 (dd, J_1 = 7.7 Hz, J_2 = 1.6 Hz, 4H, Ar), 7.26 (t, J = 7.8 Hz, 4H, Ar), 1.74 (s, 12H, 4 × CH_3); ^{13}C NMR (75 MHz, $CDCl_3$): 143.9 (C), 140.9 (C), 131.3 (C), 128.5 (CH), 123.3 (CH), 123.1 (CH), 34.2 (C), 32.7 (CH_3); ESIMS (*m/z*) [M + H] calcd for $C_{30}H_{24}O_2N_4$ 473.52, found 473.32.

Acknowledgment. We gratefully thank Dr. Midori Goto for the X-ray crystallography.

Supporting Information Available: General experimental methods; X-ray crystal data for **2(t)**, **2(c)**, **1(t,t)**, and **1(c,c)**; and ^{1}H and ^{13}C NMR spectra for structural characterization and purity of the reported compounds. This material is available free of charge via the Internet at http://pubs.acs.org.

JO0513616